



Published in final edited form as:

Nature. 2008 December 4; 456(7222): 667–670. doi:10.1038/nature07460.

Role for perinuclear chromosome tethering in maintenance of genome stability

Karim Mekhail, Jan Seebacher, Steven P. Gygi, and Danesh Moazed*

Department of Cell Biology, Harvard Medical School, Boston, Massachusetts, 02115, USA

Abstract

Repetitive DNA sequences, which constitute half the genome in some organisms, often undergo homologous recombination. This can instigate genomic instability due to gain or loss of DNA¹. Assembly of DNA into silent chromatin is generally thought to serve as a mechanism ensuring repeat stability by limiting access to the recombination machinery². Consistent with this notion, in the budding yeast *Saccharomyces cerevisiae*, stability of the highly repetitive ribosomal DNA (rDNA) sequences requires a Sir2-containing chromatin silencing complex that also inhibits transcription from foreign promoters and transposons inserted within the repeats by a process called rDNA silencing²⁻⁵. Here, we describe a protein network that stabilizes rDNA repeats of budding yeast via interactions between rDNA-associated silencing proteins and two inner nuclear membrane (INM) proteins. Deletion of either the INM or silencing proteins reduces perinuclear rDNA positioning, disrupts the nucleolus-nucleoplasm boundary, induces the formation of recombination foci, and destabilizes the repeats. In addition, artificial targeting of rDNA repeats to the INM suppresses the instability observed in cells lacking an rDNA-associated silencing protein typically required for peripheral tethering of the repeats. Moreover, in contrast to Sir2 and its associated nucleolar factors, the INM proteins are not required for rDNA silencing, indicating that Sir2-dependent silencing is not sufficient to inhibit recombination within the rDNA locus. These findings demonstrate a role for INM proteins in perinuclear chromosome localization and show that tethering to the nuclear periphery is required for rDNA repeat stability. The INM proteins studied here are conserved and have been implicated in chromosome organization in metazoans^{6,7}. Our results therefore reveal an ancient mechanism in which interactions between INM and chromosomal proteins ensure genome stability.

Users may view, print, copy, and download text and data-mine the content in such documents, for the purposes of academic research, subject always to the full Conditions of use:http://www.nature.com/authors/editorial_policies/license.html#terms

*Correspondence and requests for materials should be addressed to D.M. (danesh@hms.harvard.edu)..

Author Contributions K.M. and D.M. designed experiments and wrote the paper. K.M. and J.S. performed LC-MS/MS analyses. K.M. performed the other experiments. S.P.G. provided mass spectrometry expertise and equipment.

Author Information Reprints and permissions information is available at www.nature.com/reprints.

Full Methods and any associated references are available in the online version of the paper at www.nature.com/nature.

Supplementary Information is linked to the online version of the paper at www.nature.com/nature. A figure illustrating the molecular network studied in this paper is included in the SI (Supplementary Fig. 1).

List of key proteins (14): Lrs4, Csm1, Heh1/Src1/Yml034w, Nur1/Ydl089w, Sir2, Net1, Cdc14, Fob1, Tof2, Emerin, Man1, LAP, RNA Polymerase I, RNA Polymerase II.

Keywords

Nucleolus; rDNA; ribosomal RNA genes; copy number; unequal recombination; silencing; heterochromatin; chromosome; Heh1; Man1; Nur1; Ydl089w; CLIP; LEM domain; HEH fold; Emerin; Sir2; SIRT1; RENT; Net1; Cdc14; nuclear envelope; perinuclear; nuclear periphery

Eukaryotic rDNA is tandemly repeated anywhere from ~100 to over 10,000 times⁸. rDNA repeats provide the foundation for at least one ribosome-manufacturing compartment, the nucleolus. Budding yeast *Saccharomyces cerevisiae* has 100-200 rDNA units tandemly arranged on chromosome XII (Chr. XII) and forming one nucleolus (Fig. 1a, b)⁸. In addition to harboring rRNA-coding DNA sequences, each unit contains intergenic spacers (IGS1 and 2) that promote repeat integrity (Fig. 1a)⁹⁻¹¹. Recruitment of nucleolar protein complexes RENT (regulator of nucleolar silencing and telophase exit; composed of Cdc14, Net1/Cfi1, and Sir2) and Cohibin (mitotic monopolin proteins Lrs4 and Csm1) to IGS1 suppresses unequal recombination at the repeats^{3,12-16}. This suppression is seemingly linked to the ability of these complexes to induce rDNA silencing, which involves chromatin changes preventing RNA Polymerase II-driven transcription within IGSs of rDNA^{4,5,16-19}.

Purification of Cohibin suggested an association with INM proteins of unknown function¹⁶. To gain insight into the possible role of this association in nucleolar organization, we purified native Cohibin and INM proteins using tandem affinity purification (TAP). The TAP-tagged proteins are functional *in vivo* (Ref.16 and below). We detected purified complexes by silver staining and total protein mixtures were analyzed by liquid chromatography coupled with tandem mass spectrometry (LC-MS/MS). Negative controls were untagged cells. Purification of Lrs4 and Csm1 yielded peptides of INM proteins Heh1 (helix extension helix 1, also called Src1) and Nur1 (nuclear rim 1, Ydl089w) (Fig. 1c, d; Supplementary Table 1, part A)¹⁶. Heh1, the orthologue of human Man1, is a member of a family of INM proteins containing a highly conserved LAP-Emerin-Man1 domain (LEM, also called HEH; Supplementary Fig. 2)²⁰⁻²². LEM-domain proteins are linked to multiple clinical conditions via emerging roles in fundamental cellular processes, including gene expression and chromatin organization^{6,7,20,21,23,24}. Little is known about Heh1 and Nur1²⁰, which we define here as chromosome linkage INM proteins (CLIP). Purification of either INM protein yielded peptides for both Heh1 and Nur1 (Fig. 1e, f; Supplementary Text, section A). Purification of Heh2, an Heh1 homologue (Supplementary Fig. 2)²⁰, did not yield peptides for CLIP or Cohibin proteins (Fig. 1e, f; Supplementary Fig. 3c; Supplementary Table 1). Moreover, TAP-tagged Heh1, Lrs4, and Csm1 coimmunoprecipitated with Myc13-tagged Lrs4, Heh1, and Nur1, respectively (Supplementary Fig. 3d). Migration of Heh1 to 115 kDa, instead of the predicted 95 kDa, led us to identify multiple post-translational modifications of the protein and fluctuation of Heh1 levels over the cell cycle with peaks at interphase and mitosis (Supplementary Figs 3a, e, f, and 4). These findings physically link rDNA-associated complexes to INM proteins.

Peripheral association of genes is linked to silent chromatin assembly, which seemingly stabilizes repeats by limiting access to recombination proteins^{2,7}. Thus, CLIP may assemble at IGS1 to cooperate with RENT and Cohibin to silence transcription and inhibit unequal rDNA recombination. Therefore, we monitored unequal sister chromatid exchange (USCE)

by measuring the rate of loss of an *ADE2* marker gene from rDNA repeats. Deletion of Sir2, Lrs4, or Csm1 increased USCE, as expected (Fig. 2a, b; Supplementary Table 4)^{16,25}. USCE also increased following deletion of Heh1 or Nur1, but not Heh2 (Fig. 2a, b; Supplementary Table 4). *heh1 nur1* cells displayed additive USCE defects compared to single mutants, suggesting that INM proteins play partially overlapping roles at rDNA. Moreover, deletion of Heh1, Lrs4, or Csm1 exacerbated the effect of losing Sir2 (Fig. 2a; Supplementary Table 4)¹⁶ suggesting that Sir2 stabilizes rDNA via CLIP/Cohibin-dependent and -independent processes. Since increases in USCE affect rDNA copy-number on Chr. XII, we analyzed its size using contour-clamped homogeneous electric field (CHEF). Chr. XII measured ~2.83 Mbp in wild-type cells (~190 rDNA units) and chromosome smearing in *sir2* cells was indicative of severe changes in rDNA copy-number (Fig. 2c; Supplementary Fig. 5a), as expected^{4,17}. Interestingly, deletion of Lrs4, Csm1, Heh1, or Nur1 resulted in marked changes in rDNA copy-number averages and chromosome smearing patterns (Fig. 2c; described in Supplementary Text, section B). Together, these data suggest that the perinuclear protein network studied here is required for rDNA repeat stability.

We next studied the ability of cells to silence an RNA Pol II-transcribed *mURA3* reporter gene positioned within IGS1 or IGS2 by assessing cellular growth on synthetic complete (SC) medium that is either lacking uracil (-Ura, silencing disrupts growth) or supplemented with 5-fluoro-orotic acid (+5FOA, silencing allows growth). Deletion of Sir2, Lrs4, or Csm1 disrupted IGS1 silencing (Fig. 2d), as expected¹⁶. Surprisingly, in contrast to rDNA repeat stability, Heh1 and Nur1 were dispensable for silencing (Fig. 2d; Supplementary Fig. 5b), suggesting that silencing is insufficient for proper repeat size regulation.

We next asked whether tethering rDNA repeats to INM proteins via Cohibin limited recombination independently of silencing. Using immunofluorescence, we visualized the functional green fluorescent protein (GFP)-tagged Net1 and Myc13-tagged Heh1 (Supplementary Table 4)^{3,16}. Net1 associates with rDNA in the nucleolus throughout the cell cycle and recruits Sir2 to IGS13. However, enrichment of Sir2 at rDNA in chromatin immunoprecipitation (ChIP) experiments is unaffected by deletion of Cohibin (Supplementary Figs 1 and 8c). To measure the limit of Net1-GFP internalization, the nucleus, delineated by peripheral Heh1-Myc13 signal, was divided in three concentric zones of equal area, zone I being most peripheral²⁶. Cells were categorized according to whether the centre of the least peripheral Net1-GFP focus localizes to zone I, II, or III. Most wild-type cells displayed peripheral Net1-GFP localization (zone I, 74%) while few contained central Net1-GFP staining (zone III, 2%) (Supplementary Fig. 6a). Lrs4 or Csm1 deletion drastically shifted Net1-GFP to zone II or III (Supplementary Fig. 6a) and expanded the volume occupied by Net1-GFP within nuclear space in 3D (Fig. 3a), suggesting that optimal perinuclear localization of the rDNA-associated Net1 requires Cohibin.

How rDNA is separated from the bulk of nuclear DNA is unknown (Fig. 1b). We tested if the perinuclear network studied here affects this subnuclear separation. Nocodazole-arrested cells were analyzed by fluorescence in-situ hybridization (FISH) to visualize rDNA and 4',6-diamidino-2-phenylindole dihydrochloride (DAPI) staining to visualize bulk nuclear DNA. Wild-type cells exhibited line-shaped rDNA spooling away from the DNA bulk towards the

nuclear periphery (Fig. 3b and quantification in Supplementary Fig. 6b)27. Deletion of *Lrs4*, *Csm1*, or *Heh1*, but not *Heh2*, caused rDNA to adopt amorphous distributions often overlapping DAPI signal and a small percentage of cells exhibited two separable rDNA bodies (Fig. 3b; Supplementary Fig. 6b), which may reflect severe loss of interactions between rDNA repeats on Chr. XII sister chromatids. *Nur1* deletion caused smaller changes in rDNA morphology, which appeared less condensed (Fig. 3b; $65 \pm 6\%$ of cells, mean \pm s.d.). Disorganization of rDNA was also observed in asynchronous cells (Supplementary Fig. 6c).

We next studied the localization of a specific site within rDNA repeats in live cells harboring a *tetO* array at rDNA repeats and expressing *tetO*-binding TetI-RFP (TetI fused to red fluorescent protein) and the nucleolar Nop1-CFP (Nop1 protein fused to cyan fluorescent protein)28. TetI-RFP localized inside or at the periphery of the nucleolus in most wild-type cells (93%; Fig. 3c; Supplementary Fig. 6d, e). Deletion of *Lrs4* or *Heh1* shifted TetI-RFP outside of the nucleolus or to its periphery (Fig. 3c; Supplementary Fig. 6d, e). *sir2* cells exhibited less severe mislocalization of TetI-RFP (Fig. 3c; Supplementary Fig. 6d, e). Deletion of *Lrs4*, *Heh1*, or *Sir2* also induced the formation of extranucleolar DNA repair centers, as marked by clustering of the yellow fluorescent protein-tagged Rad52 recombination protein, Rad52-YFP (Fig. 3c; Supplementary Fig. 6d, f). Fewer *sir2* cells exhibited Rad52 foci compared to *heh1* or *lrs4* cells (Supplementary Fig. 6f). This is in contrast to USCE in *sir2* cells, which is higher than that of *heh1* or *lrs4* cells (Fig. 2a), suggesting that more recombinations in *sir2* cells are unequal crossovers. Alternatively, a higher incidence of Rad52-YFP foci in cells lacking *Heh1* or *Lrs4* might suggest that these proteins stabilize several genetic loci. Most Rad52-YFP foci (61%-65%) did not overlap TetI-RFP signal in *lrs4*, *heh1*, or *sir2* cells (Fig. 3c; Supplementary Fig. 6d, f), likely reflecting the occurrence of one or few repair events per rDNA array and their distance from *tetO* sequences. While we cannot exclude the possibility that the *tetO* array contributes to rDNA mislocalization in *lrs4*, *heh1*, or *sir2* cells, disruption of rDNA organization in *lrs4* and *heh1* cells lacking *tetO* sites, as revealed by FISH and immunofluorescence (Fig. 3a, b; Supplementary Fig. 6a-c), argues against this possibility and suggests that the perinuclear complexes studied here help stabilize wild-type rDNA repeats. Together, these results suggest that *Heh1* and *Lrs4*, and to a lesser extent *Sir2*, are required for sequestration of rDNA in the peripherally located nucleolus, and show that loss of sequestration correlates with increased repeat instability (Fig. 2) and Rad52 recombination foci.

To further analyze CLIP-Cohibin links, we performed ChIP using a combination of dimethyl adipimidate and formaldehyde crosslinkers. We observed 2.85 ± 0.37 and 2.35 ± 0.12 fold enrichments for IGS1 sequences in *Lrs4*-TAP and *Heh1*-TAP immunoprecipitations, respectively (Fig. 3d, e; Supplementary Fig. 7). We did not detect an enrichment using *Nur1*-TAP, likely due to its low abundance or weaker association with Cohibin (Fig. 3d; Supplementary Figs 3a and 7a-c). More importantly, deletion of *Lrs4* abolished the IGS1 enrichment of *Heh1*-TAP without affecting its levels (Fig. 3e; Supplementary Fig. 7d-f). In contrast, no enrichment was detected for *Heh2*-TAP (Fig. 3e; Supplementary Fig. 7d), an INM protein that neither interacts with Cohibin (Fig. 1) nor affects rDNA stability (Fig. 2), although expressed to similar levels as *Heh1* (data not shown)29. Together, these data

indicate that CLIP/Cohibin-mediated tethering of rDNA repeats to the INM is required for repeat stability.

To determine if perinuclear tethering suppresses recombination in the absence of Cohibin proteins, which are required for rDNA silencing and suppression of recombination, we created a strain in which rDNA was linked to Heh1 via Sir2. We fused *HEH1* and *SIR2* genes in *lrs4* cells creating a hybrid *HEH1-SIR2* gene (Fig. 4a). This yielded a fusion protein of expected size (~175 kDa) detectable in anti-Sir2 immunoblotting (Supplementary Fig. 8a). Fusion of Heh1 and Sir2 restored the separation of rDNA from bulk nuclear DNA in *lrs4* cells (Fig. 4b), reduced unequal recombination (Fig. 4c; Supplementary Table 4), and increased homogeneity in the size of Chr. XII in cell populations (Fig. 4d; Supplementary Fig. 8b). Furthermore, ChIP revealed that Heh1-Sir2 associated with rDNA to similar levels as Sir2 (Supplementary Fig. 8c). Moreover, Heh1-Sir2 did not rescue IGS1-specific increases in histone H3 acetylation, a marker for loss of silencing, caused by *Lrs4* deletion (Supplementary Fig. 8c). The inability of Heh1-Sir2 to fully restore rDNA stability may be due to other *Lrs4* functions, such as silencing or perhaps chromosome condensation, which suppress recombination at repeats. Attempts to fuse Heh1 with other perinuclear proteins, such as Tof2 or Ku70, did not yield viable cells (data not shown). Thus, tethering rDNA to the INM can promote repeat stability at least partially independently of silencing.

Our results suggest that Sir2-dependent silencing alone cannot inhibit recombination within the repetitive rDNA locus and that INM-mediated perinuclear chromosome tethering ensures repeat stability (Fig. 4e; Supplementary Fig. 1). Extranucleolar Rad52 focus formation in *lrs4*, *heh1*, or *sir2* cells concurs with suggestions that while early rDNA recombination steps occur inside the nucleolus, Rad52 sumoylation and a high local concentration of the Smc5-Smc6 complex preclude Rad52 focus formation within nucleolar space²⁸. Thus, our findings suggest that rDNA repeats unleashed from the INM accumulate lesions that can better access the nucleoplasm where high concentrations of functional Rad52 promote DNA repair by homologous recombination. Therefore, perinuclear tethering likely sequesters repeats away from recombination factors and may be required for Cohibin and RENT to stably align rDNA sister chromatids during replication to prevent unequal crossovers (Fig. 4e). Recombination between homologous repeats dispersed in the genome often instigates catastrophic chromosomal rearrangements. We anticipate that proteins studied here are members of perinuclear networks that control recombination at multiple loci to maintain genome stability.

Methods Summary

Standard co-immunoprecipitations^{3,14}, ChIP¹⁴, TAP purification¹⁶, immunofluorescence¹⁶, rDNA silencing¹⁶, USCE¹⁶, FISH²⁷, and live cell²⁸ assays were performed as previously described. Modified ChIP (employing both formaldehyde and dimethyl adipimidate crosslinkers) and modified TAP purifications (employing different detergents) are described in Methods. Information about strain construction, materials, LC-MS/MS, CHEF, microscopy/imaging, whole-cell protein analysis, and cell-cycle arrest is available in Methods.

Supplementary Material

Refer to Web version on PubMed Central for supplementary material.

Acknowledgements

We thank Calvin Yip, Tom Walz, Julie Huang, Marc Bühler, Adam Rudner, Vincent Guacci, Douglas Koshland, Alexander Palazzo, Diana E. Libuda, Fred Winston, Lidia Vasiljeva, Stephen Buratowski, John E. Warner, Christine Anderson, Gerald A. Beltz, Michael Lisby, Tom Daniel, Lai Ding, and the Harvard NeuroDiscovery Optical Imaging Center for technical assistance or materials; Tom Rapoport, Tetsushi Iida, Mohammad Motamedi, Aaron Johnson, Megumi Onishi, Erica Gerace, Shane Buker, Mario Halic and members of the Moazed laboratory for helpful discussions and comments. We were not able to cite many original studies due to space limitations. This work was supported by grants from the National Institutes of Health (D.M.) and Canadian Institutes of Health Research Institute of Aging (K.M.). D.M. is a scholar of the Leukemia and Lymphoma Society.

Appendix

Methods

Strains and materials

Endogenous genes were deleted or modified with C-terminal epitope tags as described^{14,16}. Strains harboring *mURA3* reporter genes were described¹⁴. For Heh1-Sir2 fusion, *HEH1* was amplified with its promoter from genomic DNA using primers KM11 (GATAactagtTTCTGCCTGTAGAGAGAG) and KM12 (GATAgggcccCAAATATGGCAACT CGGA). SpeI/ApaI-digested products were ligated into pRS314 yielding a plasmid used as template to amplify *HEH1* with the upstream *TRP1* gene using primers KM14 (CATTCAAACCATTTTTCCCTCATCGGCACATTAAGCTGGATGTCTGTTATTAAT TTCAC) and KM17 (CGCTAGTCTTTGATACGGCGTATTCATATGTGGGATGGTTATTTGTTTTTCAGC GGAAT) adding regions flanking endogenous *SIR2* start site. Cells lacking the endogenous *HEH1* ORF, transformed with PCR products, and selected on -TRP medium, were PCR/immunoblotting-screened. Antibodies: anti-myc-9E10 (Covance), anti-Actin (Millipore), HRP-conjugated anti-TAP or anti-Myc (Invitrogen), anti-digoxin (Jackson Laboratories), anti-AcK9/AcK14 H3 (Millipore), anti-CBP (Open Biosystems), anti-Cyclin-B2 and anti-GFP (Adam Rudner, University of Ottawa), Rhodamine-tagged goat anti-mouse (Jackson Laboratories), Alexa488-labelled goat anti-rabbit (Molecular Probes), FITC-conjugated goat anti-mouse (Jackson Laboratories), FITC-conjugated swine anti-goat (Invitrogen), anti-Sir230.

Protein purifications

Standard assays were done as described¹⁶. Purifications incorporating CHAPS were performed as described¹⁶ with modifications: (I) 1% CHAPS was added to lysis and TEV-cleavage buffers. (II) 0.05% CHAPS was added to CAM binding and elution buffers. (III) Regarding purified mixtures, 10-50% was submitted to electrophoresis/silver staining and half was TCA-precipitated for spectrometric analysis.

Mass spectrometry

Trypsin-digested mixtures were subjected to LC-MS/MS³¹ and MS/MS spectral analysis³² as described (<1% false positive rate). Proteins in untagged controls were removed. Spectral counts semi-quantitatively measuring the relative abundance of proteins are in Supplementary Tables 2 and 3. Excised gel bands were minced, destained, dehydrated, and trypsin-digested before extraction of digests. Modifications were identified with SEQUEST Sorcerer (Sage-N Research) allowing variable methionine oxidation, serine/threonine phosphorylation, and lysine ubiquitylation. Only unambiguous phosphosites³³ are reported.

FISH

Experiments were conducted as described²⁷. rDNA probes were a gift from Vincent Guacci (Carnegie Institution) or were prepared from Bgl-II fragments from plasmids p362 and p363, which contain the 5' and 3' half of an rDNA unit, respectively, using the BioNick (Invitrogen) and Digoxigenin (Roche) labeling systems²⁷. Scoring was conducted at the microscope and representative images adjusted for contrast/coloring are shown.

Imaging

Images were collected with an Axiovert200 microscope (Carl Zeiss) coupled to an EM-CCD digital camera (Hamamatsu Photonics) or an Eclipse 80i microscope (Nikon). GFP spot positions were determined as described²⁶. The outer circle was set to coordinates where the red signal shows the largest intensity drop, moving centrally, as revealed by ImageJ (NIH). Scoring and measurements were conducted with Metamorph (Molecular Devices) and representative images were adjusted for background using levels/contrast in Photoshop (Adobe). Other software programs handling data were Office (Microsoft) and FreeHand (Macromedia).

3D reconstruction

Average of four images for each of ~15 Z sections were generated using Zeiss LSM510 (Carl Zeiss) upright confocal microscope (Harvard NeuroDiscovery Optical Imaging Center). Respective settings for red and green signals: LP-560 and LP-505 emission, 543 and 488 excitation, 50 and 62 pinhole. Constant background corrections were done in ImageJ (NIH). Reconstruction was done with volume tools of Imaris (Bitplane).

ChIP

Standard ChIP (Supplementary Fig. 8) was conducted as described¹⁴. Modified ChIP (Fig. 3; Supplementary Fig. 7) was conducted as described^{14,16} with protein-protein crosslinkers added³⁴. Modifications are as follows: Yeast cultures (50 ml) were grown to OD₆₀₀ ~0.8. Cells were centrifuged, washed with ice-cold phosphate buffer saline (PBS), suspended in 10 ml ice-cold/fresh protein-protein crosslinking solution (10 mM DMA and 0.25% dimethyl sulfoxide in PBS) and nutated at room temperature (RT, 45 min). PBS-washed cells were resuspended in 50 ml of 1% formaldehyde in PBS (11 h), then Glycine was added to 125 mM. PBS-washed cells were resuspended in 400 µl of lysis buffer, subjected to bead-beating, and procedures were continued as described^{14,16} except that RNase was added prior to proteinase K. Dilutions for IP and input DNA were 1:2 and 1:20,000, respectively.

[α - ^{32}P]-dCTP-labeled and EtBr-stained products were quantified with Molecular Imager/QuantityOne (Bio-Rad) and Image ReaderLAS-3000/ImageGauge (Fuji), respectively.

USCE

Assays were essentially performed as described^{16,25}. Cells were grown to OD₆₀₀ 0.4-0.8, sonicated briefly, and spread (~400 cells/plate) on thick plates (5 mg/L adenine). Incubation was 30°C/5 days, 4°C/2 days, then RT/3 days. Rates were obtained by dividing the number of half-sectored colonies by the total number of colonies excluding completely red colonies.

CHEF and Southern

Experiments were conducted as described^{11,35,36} with modifications. 1 ml of saturated overnight culture was washed and suspended in 300 μl EDTA/Tris (50 mM EDTA/10 mM Tris-HCl pH 7.5). 2 μl zymolyase (20 $\mu\text{g}/\mu\text{l}$ in 10 mM Na₂HPO₄ pH 7.5) and 500 μl low melting point CHEF quality agarose (1% in 125 μM EDTA pH 8.0, 42°C; Bio-Rad) were added and the mixture solidified in plug molds at 4°C. Plugs were incubated in 1 ml of 10 μM Tris-HCl pH7.5, 500 μM EDTA at 37°C overnight then in 1 ml of 2 mg/ml proteinase K in 10 μM Tris-HCl pH7.5, 500 μM EDTA, 10 mg/ml N-lauroylsarcosine at 50°C overnight. Plugs were washed three times with EDTA/Tris (4°C, 1 h/wash) and stored in 2 ml EDTA/Tris (4°C). Plugs were prepared at 5-3-1.5 mm and run (68 h, 3.0 V/cm, 300-900 s, 10°C) on a 0.8% CHEF agarose gel in 0.5X TBE/CHEF-DR-II (Bio-Rad). CHEF size markers were *Hansenula wingei* chromosomes (Bio-Rad). EtBr-stained gels were imaged then submitted to standard Southern blotting. Blots were UV-crosslinked and probed (65°C, 16 h) with ^{32}P -dCTP-labeled IGS1.

Whole cell protein preparation

Lysates were prepared by bead-beating¹⁶ except for Supplementary Fig. 8a, where they were prepared by TCA-coupled lysis as Heh1-Sir2 was otherwise unstable. For this, 2×10^7 cells grown to OD₆₀₀ ~0.75 were washed and suspended in 500 μl ice-cold water. Sequential additions of 75 μl of alkali/ β -ME (1.85 N NaOH, 1.065 M β -ME) and 75 μl 50% TCA solutions were each followed by a 10 min incubation on ice. After centrifugation (10,000 rpm/4°C/10 min), pellets were suspended in loading buffer (1X standard loading buffer, 1.42 M β -ME, 83.2 mM Tris-HCl pH 8.8), boiled and supernatants were saved.

α -factor arrest

Cells grown to OD₆₀₀ 0.2 were incubated 3 h with α -factor (10 $\mu\text{g}/\text{ml}$). Cells were washed, resuspended in fresh media and samples collected every 15 min were frozen in liquid nitrogen.

References

30. Moazed D, Johnson D. A deubiquitinating enzyme interacts with SIR4 and regulates silencing in *S. cerevisiae*. *Cell*. 1996; 86:667–677. [PubMed: 8752220]
31. Haas W, et al. Optimization and use of peptide mass measurement accuracy in shotgun proteomics. *Mol. Cell. Proteomics*. 2006; 5:1326–1337. [PubMed: 16635985]

32. Buker SM, et al. Two different Argonaute complexes are required for siRNA generation and heterochromatin assembly in fission yeast. *Nat. Struct. Mol. Biol.* 2007; 14:200–207. [PubMed: 17310250]
33. Beausoleil SA, Villen J, Gerber SA, Rush J, Gygi SP. A probability-based approach for high-throughput protein phosphorylation analysis and site localization. *Nat. Biotechnol.* 2006; 24:1285–1292. [PubMed: 16964243]
34. Kurdistani SK, Grunstein M. In vivo protein-protein and protein-DNA crosslinking for genomewide binding microarray. *Methods.* 2003; 31:90–95. [PubMed: 12893178]
35. Oakes M, Siddiqi I, Vu L, Aris J, Nomura M. Transcription factor UAF, expansion and contraction of ribosomal DNA (rDNA) repeats, and RNA polymerase switch in transcription of yeast rDNA. *Mol. Cell. Biol.* 1999; 19:8559–8569. [PubMed: 10567580]
36. Libuda DE, Winston F. Amplification of histone genes by circular chromosome formation in *Saccharomyces cerevisiae*. *Nature.* 2006; 443:1003–1007. [PubMed: 17066037]

References

1. Szostak JW, Wu R. Unequal crossing over in the ribosomal DNA of *Saccharomyces cerevisiae*. *Nature.* 1980; 284:426–430. [PubMed: 6987539]
2. Moazed D. Common themes in mechanisms of gene silencing. *Mol. Cell.* 2001; 8:489–498. [PubMed: 11583612]
3. Straight AF, et al. Net1, a Sir2-associated nucleolar protein required for rDNA silencing and nucleolar integrity. *Cell.* 1999; 97:245–256. [PubMed: 10219245]
4. Bryk M, et al. Transcriptional silencing of Ty1 elements in the RDN1 locus of yeast. *Genes Dev.* 1997; 11:255–269. [PubMed: 9009207]
5. Smith JS, Boeke JD. An unusual form of transcriptional silencing in yeast ribosomal DNA. *Genes Dev.* 1997; 11:241–254. [PubMed: 9009206]
6. Capell BC, Collins FS. Human laminopathies: nuclei gone genetically awry. *Nat. Rev. Genet.* 2006; 7:940–952. [PubMed: 17139325]
7. Reddy KL, Zullo JM, Bertolino E, Singh H. Transcriptional repression mediated by repositioning of genes to the nuclear lamina. *Nature.* 2008; 452:243–247. [PubMed: 18272965]
8. Nomura M. Ribosomal RNA genes, RNA polymerases, nucleolar structures, and synthesis of rRNA in the yeast *Saccharomyces cerevisiae*. *Cold Spring Harb. Symp. Quant. Biol.* 2001; 66:555–565. [PubMed: 12762057]
9. Keil RL, Roeder GS. Cis-acting, recombination-stimulating activity in a fragment of the ribosomal DNA of *S. cerevisiae*. *Cell.* 1984; 39:377–386. [PubMed: 6094015]
10. Brewer BJ, Fangman WL. A replication fork barrier at the 3' end of yeast ribosomal RNA genes. *Cell.* 1988; 55:637–643. [PubMed: 3052854]
11. Kobayashi T, Ganley AR. Recombination regulation by transcription-induced cohesin dissociation in rDNA repeats. *Science.* 2005; 309:1581–1584. [PubMed: 16141077]
12. Visintin R, Hwang ES, Amon A. Cfi1 prevents premature exit from mitosis by anchoring Cdc14 phosphatase in the nucleolus. *Nature.* 1999; 398:818–823. [PubMed: 10235265]
13. Shou W, et al. Exit from mitosis is triggered by Tem1-dependent release of the protein phosphatase Cdc14 from nucleolar RENT complex. *Cell.* 1999; 97:233–244. [PubMed: 10219244]
14. Huang J, Moazed D. Association of the RENT complex with nontranscribed and coding regions of rDNA and a regional requirement for the replication fork block protein Fob1 in rDNA silencing. *Genes Dev.* 2003; 17:2162–2176. [PubMed: 12923057]
15. Rabitsch KP, et al. Kinetochore recruitment of two nucleolar proteins is required for homolog segregation in meiosis I. *Dev. Cell.* 2003; 4:535–548. [PubMed: 12689592]
16. Huang J, et al. Inhibition of homologous recombination by a cohesin-associated clamp complex recruited to the rDNA recombination enhancer. *Genes Dev.* 2006; 20:2887–2901. [PubMed: 17043313]
17. Gottlieb S, Esposito RE. A new role for a yeast transcriptional silencer gene, SIR2, in regulation of recombination in ribosomal DNA. *Cell.* 1989; 56:771–776. [PubMed: 2647300]

18. Fritze CE, Verschueren K, Strich R, Easton Esposito R. Direct evidence for SIR2 modulation of chromatin structure in yeast rDNA. *EMBO J.* 1997; 16:6495–6509. [PubMed: 9351831]
19. Smith JS, Caputo E, Boeke JD. A genetic screen for ribosomal DNA silencing defects identifies multiple DNA replication and chromatin-modulating factors. *Mol. Cell. Biol.* 1999; 19:3184–3197. [PubMed: 10082585]
20. King MC, Lusk CP, Blobel G. Karyopherin-mediated import of integral inner nuclear membrane proteins. *Nature.* 2006; 442:1003–1007. [PubMed: 16929305]
21. Brachner A, Reipert S, Foisner R, Gotzmann J. LEM2 is a novel MAN1-related inner nuclear membrane protein associated with A-type lamins. *J. Cell Sci.* 2005; 118:5797–5810. [PubMed: 16339967]
22. Rodriguez-Navarro S, Igual JC, Perez-Ortin JE. SRC1: an intron-containing yeast gene involved in sister chromatid segregation. *Yeast.* 2002; 19:43–54. [PubMed: 11754482]
23. Hellemans J, et al. Loss-of-function mutations in LEMD3 result in osteopoikilosis, Buschke-Ollendorff syndrome and melorheostosis. *Nat. Genet.* 2004; 36:1213–1218. [PubMed: 15489854]
24. Bione S, et al. Identification of a novel X-linked gene responsible for Emery-Dreifuss muscular dystrophy. *Nat. Genet.* 1994; 8:323–327. [PubMed: 7894480]
25. Kaerberlein M, McVey M, Guarente L. The SIR2/3/4 complex and SIR2 alone promote longevity in *Saccharomyces cerevisiae* by two different mechanisms. *Genes Dev.* 1999; 13:2570–2580. [PubMed: 10521401]
26. Gartenberg MR, Neumann FR, Laroche T, Blaszczyk M, Gasser SM. Sir-mediated repression can occur independently of chromosomal and subnuclear contexts. *Cell.* 2004; 119:955–967. [PubMed: 15620354]
27. Guacci V, Hogan E, Koshland D. Chromosome condensation and sister chromatid pairing in budding yeast. *J. Cell Biol.* 1994; 125:517–530. [PubMed: 8175878]
28. Torres-Rosell J, et al. The Smc5-Smc6 complex and SUMO modification of Rad52 regulates recombinational repair at the ribosomal gene locus. *Nat. Cell Biol.* 2007; 9:923–931. [PubMed: 17643116]
29. Ghaemmaghami S, et al. Global analysis of protein expression in yeast. *Nature.* 2003; 425:737–741. [PubMed: 14562106]

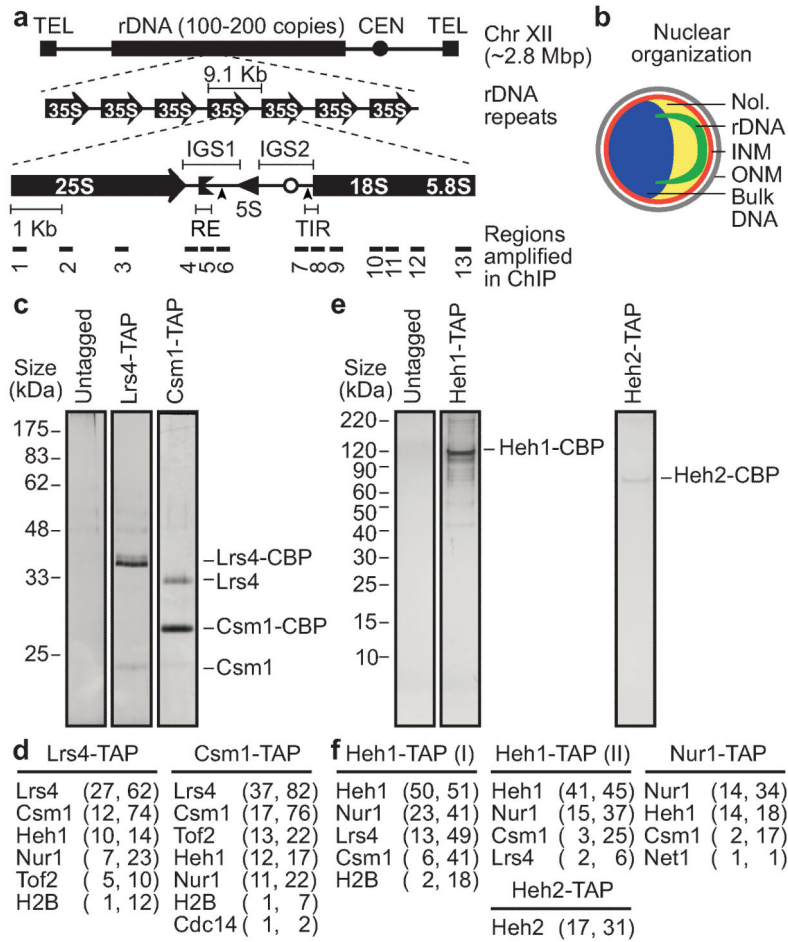


Figure 1. Protein network extending from rDNA to the nuclear envelope
a, rDNA repeats on Chr. XII. Each unit yields a Pol I-transcribed 35S precursor rRNA (processed into 25S, 18S, and 5.8S) and a Pol III-transcribed 5S rRNA. CEN, centromere; TEL, telomere; IGS, intergenic spacer; RE, recombination enhancer; replication fork block; TIR, Pol I transcription initiation region; O, DNA replication origin; Mbp, megabase pairs. Vertical arrowheads indicate insertion sites of *mURA3* reporter genes used in this study. **b**, Nuclear organization at the G₂/M cell cycle stage. No1., nucleolus; ONM, outer nuclear membrane. **c-f**, Purification of native complexes. **c, e**, Protein detection in silver-stained gels. TAP cleavage during protein purification leaves a calmodulin binding protein (CBP) fragment. **d, f**, LC-MS/MS analysis. Number of unique peptides followed by percent coverage of the protein sequence is shown. SI contains full protein lists (Supplementary Table 1, part A) and spectral counts (Supplementary Tables 2 and 3).

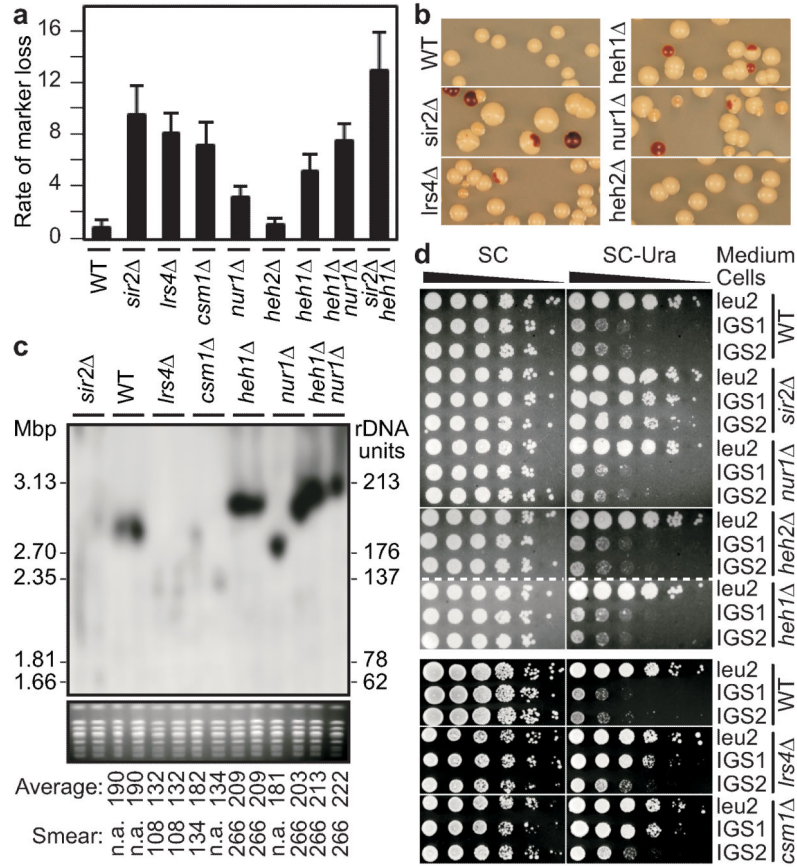


Figure 2. Role of perinuclear protein network at rDNA repeats

a, b, Rates of *ADE2* marker loss (mean ± s.d.) relative to wild-type (WT) (**a**) and representative colonies (**b**) are shown. **c**, CHEF analysis of rDNA stability. Chromosomes resolved by CHEF were probed with IGS1 rDNA (Chr. XII, top). Ethidium bromide (EtBr) staining of Chr. IV and smaller chromosomes shows quality of the preparation (bottom). Values corresponding to rDNA copy-number averages and smear edges are indicated. Chr. XII size for *sir2Δ* was too heterogeneous to estimate copy-number. **d**, Unlike Sir2 and Cohibin, CLIP is dispensable for rDNA silencing. Ten-fold serial dilutions of cells with the *mURA3* reporter gene inserted at IGS1/IGS2 (see Fig. 1a for locations) or outside rDNA at the *LEU2* locus are shown.

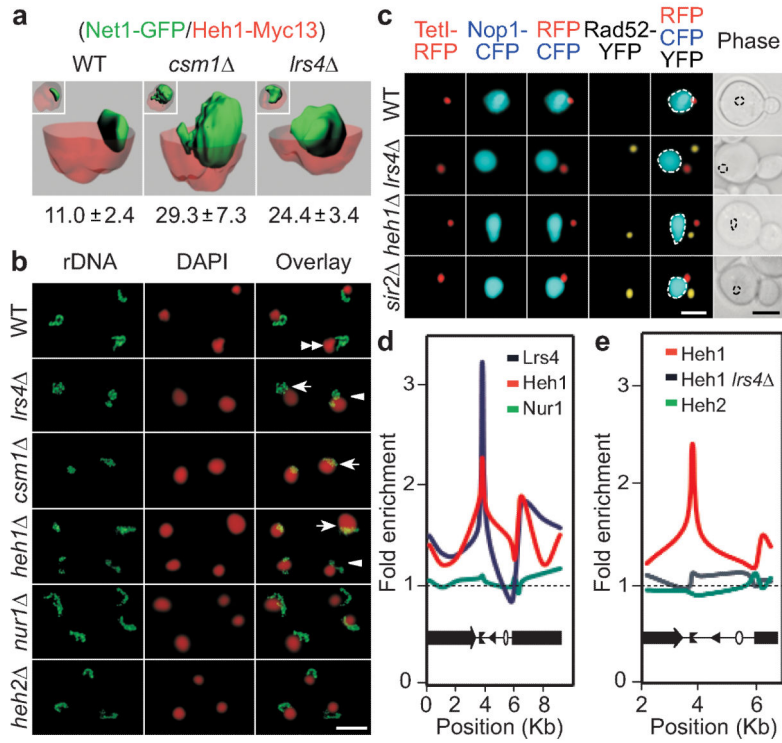


Figure 3. Protein network tethers rDNA to the nuclear envelope

a, Representative 3D reconstructions of cells from double immunofluorescence analysis reveal the relative organization of Net1-GFP (green) and Heh1-Myc13 (red). Signal boundaries are shown with clipping planes for Heh1-Myc13. Percentages of green relative to full red volumes are shown (mean ± s.d.; n = 5). **b**, Nocodazole-arrested (G₂/M) cells were subjected to FISH to visualize rDNA and DAPI staining (pseudocoloured red) to visualize bulk nuclear DNA. Cells with different rDNA morphologies are indicated by double arrowheads (spooled lines), arrows (amorphous), or triangles (two bodies) with quantifications in Supplementary Fig. 6b. Scale bar, 3 μm. **c**, Live cells with TetI-RFP-marked rDNA and expressing Rad52-YFP and nucleolar Nop1-CFP were imaged. Images depicting most observed phenotypes are shown. More images and quantifications are in Supplementary Fig. 6d-f. Scale bars are 1 μm (white) and 3 μm (black). **d**, **e**, Relative fold enrichment of indicated TAP-tagged proteins are shown. rDNA organization schematics are shown on graphs. Gels for **d** and **e** are shown in Supplementary Figs 7a and 7d, respectively. Detailed IGS1 ChIP is shown in Supplementary Fig. 7b, c.

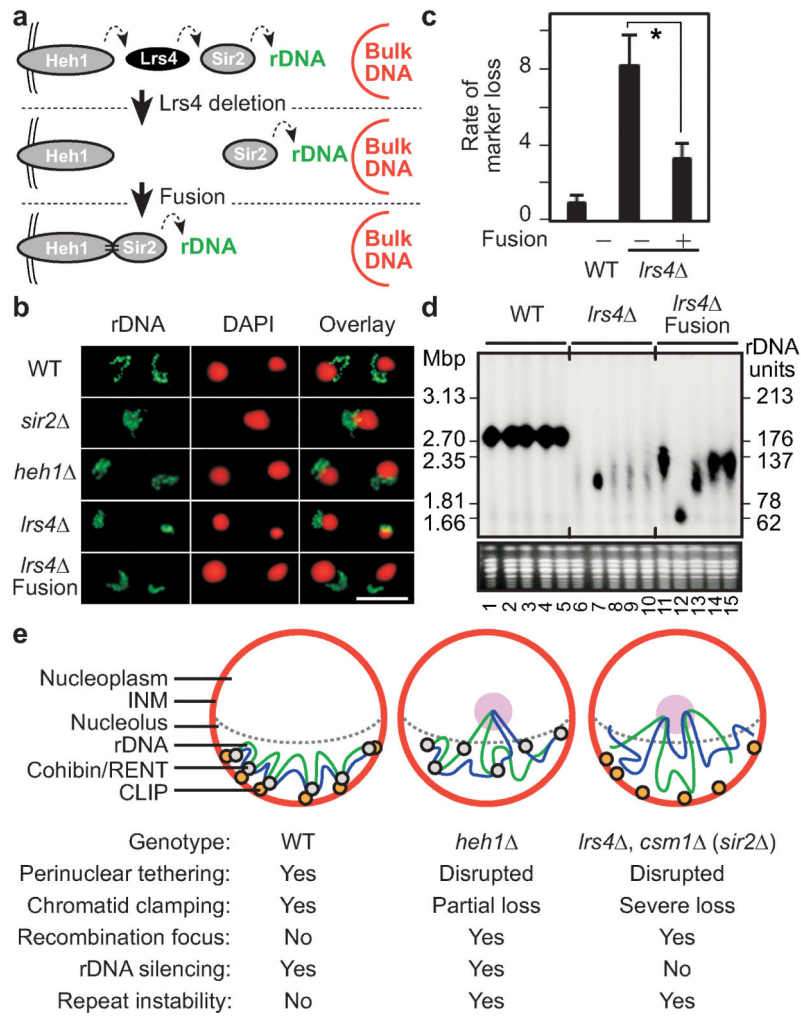


Figure 4. Targeted perinuclear tethering promotes rDNA repeat stability
a, Fusion of Heh1 to Sir2 in *lrs4* cells. Heh1 is shown embedded in the INM. **b**, FISH reveals that fusion of Heh1 and Sir2 restores the separation of rDNA signal from DAPI staining in nocodazole-arrested cells lacking Lrs4. Scale bar, 3 μ m. **c**, Relative rates of *ADE2* marker loss (mean \pm s.d.). Asterisk, $P < 0.0001$ for Student's *t* test. **d**, CHEF analysis of rDNA stability. Chromosomes resolved by CHEF were probed with IGS1 rDNA (Chr. XII, top). EtBr staining of Chr. IV and smaller chromosomes shows quality of the preparation (bottom). **e**, Functional organization of the perinuclear molecular network tethering rDNA to the nuclear periphery. Repeat instability results from the loss of either the INM CLIP proteins or rDNA silencing complexes.